ELSEVIER

Journal of Photochemistry and Photobiology A: Chemistry 124 (1999) 23–28

Journal of Photochemistry and Photobiology A:Chemistry

Heavy metal ions detection in solution, in sol–gel and with grafted porphyrin monolayers

D. Delmarre*, R. Méallet[1], C. Bied-Charreton, R.B. Pansu

PPSM (URA 1906 CNRS), ENS de Cachan, 61, avenue du Pdt Wilson, 94235 Cachan Cedex, France

Received 26 November 1998; accepted 25 January 1999

Abstract

The detection of heavy metal ions – Hg^{2+}, Pb^{2+}, Cd^{2+} – by a free base porphyrin, 5,10,15,20-tetra(4-*N*-methylpyridyl)porphyrin (TMPyP), was studied. The porphyrin was either adsorbed in sol–gel matrix (TMOS) or grafted on glass surfaces. Detection limit was 10^{-7} mol/l for mercury and cadmium, and 10^{-5} mol/l for lead. Apparent association constants were calculated at pH=7: p*K* (Cd^{2+})=−5.2; p*K* (Pb^{2+})=−4; and at pH=4 p*K* (Hg^{2+})=−5.7. Both the shift of the Soret band and the change in fluorescence lifetime enabled the identification of the metal ions.

In sol–gel, detection limits were found to be 10^{-3} mol/l but 90% of the metal salts were trapped by the matrix. In sol–gel we have shown that the ions were pumped by the matrix at a concentration of 1.5×10^{-5} mol/ml of sol–gel. The sol–gel limits both the reaction time and the detection threshold. No such effect is observed for grafted monolayers. A reaction time of 30 min and a detection limit of 10^{-6} mol/l were measured for Hg^{2+} salts.

Keywords: Porphyrin; Sol–gel; Multi-layer; Heavy metal; Sensor

1. Introduction

It is of great relevance to detect pollutants, such as heavy metal ions, for environmental purpose. Atomic absorption spectrometry and voltametry allow to detect selectively and quantitatively metal ions such as Hg^{2+}, Pb^{2+} [1]. Nevertheless these methods are expensive and cannot be used in the field. So simpler detection methods for metal ions should be investigated such as change in colour. We have studied porphyrins as probe molecules in different materials and their application to chemical sensing [2]. Porphyrins are versatile molecules whose physicochemical properties can be adjusted by modifications of the electronic distribution on the aromatic ring. They can serve as probes to study the environment. Porphyrins are known to be sensitive to metal ions [3–6]. Both absorption and fluorescence change under complexation of ions such as mercury, lead, cadmium. As reported previously [7] the immobilization of 5,10,15,20-tetra(4-*N*-sulfonatedphenyl)porphyrin (TPPS) results in an optochemical sensor for Cd^{2+} and Hg^{2+}. Such immobilization has been carried out on polymeric matrix [8] and sol–gel [9]. Immobilization of porphyrins in sol–gel materials has been reported in literature especially for applications in catalysis [10], non-linear optics [11,12], hole-burning [13,14], and sensors [15–17]. TMPyP – 5,10,15,20-tetra(4-*N*-methylpyridyl)porphyrin – has been preferred to other porphyrins because it is not leaked out of the matrix [9]. In this study we report absorption, steady-state fluorescence and time-resolved fluorescence experiments on TMPyP in solution and immobilized in sol–gel. Finally we designed a new monolayer structure of 5,10,15,20-tetra-(4-pyridine)porphyrin (TPyP) inspired by Dequan Li's work [18] we report Hg^{2+} detection. Time-response, detection limits were investigated.

2. Experimental

2.1. Reagents

All metal ions were acetates of analytical grade (Aldrich). They were solubilized in a doubly distilled water, except Hg^{2+} which was used in a buffer solution (pH=4, Britton–Robinson). TMPyP and TPyP (Fig. 1) were synthesized as described by Pasternack and coworkers [19]. The solid TMPyP was solubilized in a phosphate buffer pH=7 (Aldrich). TPyP monolayer (Fig. 2) was synthesized as described by Dequan Li [20].

*Corresponding author. E-mail: delmar@ppsm.ens-cachan.fr

[1]rachelm@ppsm.ens-cachan.fr

1010-6030/99/$ – see front matter
PII: S1010-6030(99)00046-5

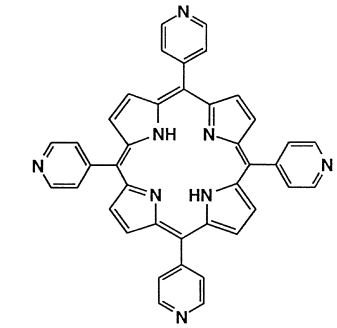

TPyP

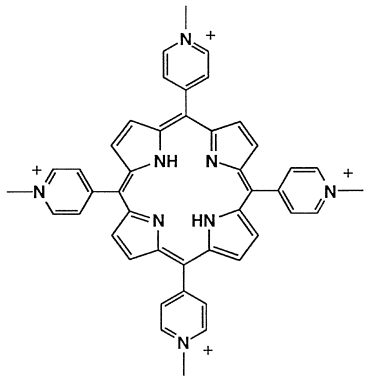

TMPyP

Fig. 1. TPyP and TMPyP structures.

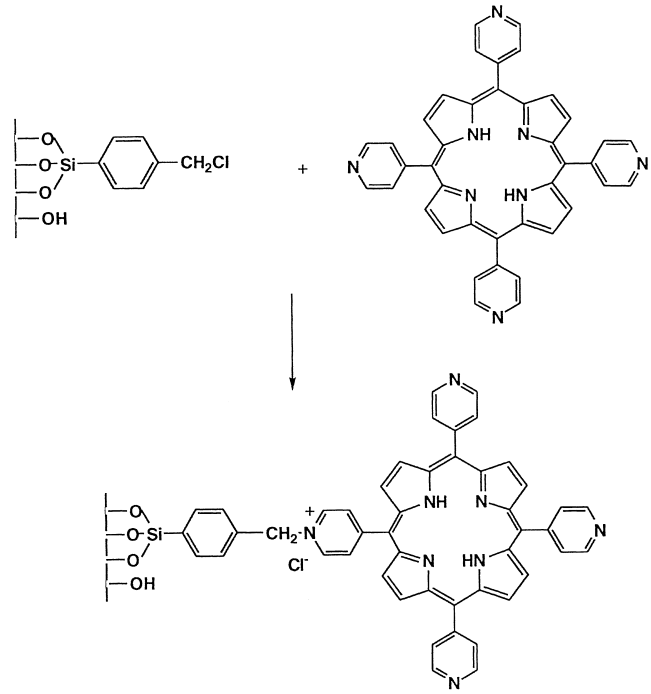

Fig. 2. TPyP monolayer: structure.

We used quartz cuvets washed with sulfochromic acid and rinsed thoroughly with water. The TMPyP solutions used were 10^{-6}–10^{-7} mol/l.

2.2. Sensing material preparation

Sol–gel materials were synthesized following the method described by Devreux et al. [21]. In a typical preparation of monolith, 15.22 g of a solution of tetramethoxysilane (TMOS) in 3.6 g of acidic water (HCl,pH=2.6) were sonicated during 15 min. An homogeneous solution (sol) is obtained. To the sol are added 24 ml of a solution of TMPyP (concentration=10^{-6} mol/l). This mixture is then placed in disposable cuvets. After 1 week a transparent solid and failure less monoliths were obtained with a parallelopiped shape and a thickness of ca 1 cm. They are stored at 3°C to stop the polymerization reaction.

2.3. Material and method

Absorption experiments were carried out on a Varian Cary 05E spectrophotometer.

Fluorescence spectra were measured on a Jobin–Yvon Spex. Fluorescence excitation was 433 nm (absorption maximum of TMPyP) and emission was collected from 550 to 800 nm.

Time-resolved experiments have been achieved with a Ti–Sa laser equiped with a single-photon counting system [22]. Excitation wavelength was 433 nm, as previously, fluorescent light was collected with a monochromator at 710 nm in solution and sol–gel.

3. Results and discussion

3.1. Experiments in solution

3.1.1. Determination of the stability constant of Hg–TMPyP complex, detection limits and lifetimes

The aqueous solution of TMPyP, at pH=4, ionic strength 0.1 mol/l, and temperature of 25°C presents maxima at 422, 520, 557, 587 and 640 nm. By addition of an excess of Hg^{2+} the colour of the solution changes from pink to green and the resulting spectrum shows an absorption maximum at 444 nm.

The stoichiometry is verified to be 1:1.

$$\mathrm{TMPyP} + \mathrm{Hg}^{2+} \Leftrightarrow \mathrm{HgTMPyP}$$

$$K(\mathrm{Hg}^{2+}) = \frac{[\mathrm{HgTMPyP}]}{[\mathrm{Hg}^{2+}][\mathrm{TMPyP}]},$$

where $K(\mathrm{Hg}^{2+})$ is the apparent equilibrium constant of the reaction and $[\mathrm{Hg}^{2+}]$ and [TMPyP] denote the equilibrium concentration of Hg^{2+} and TMPyP, respectively.

Aliquots of Hg^{2+} were added to the TMPyP solution, we can observe the disappearance of the 422 nm band and the appearance of the 444 nm band (Fig. 3). The percentage of Hg–TMPyP complex and the percentage of free base TMPyP can be determined by main component analysis

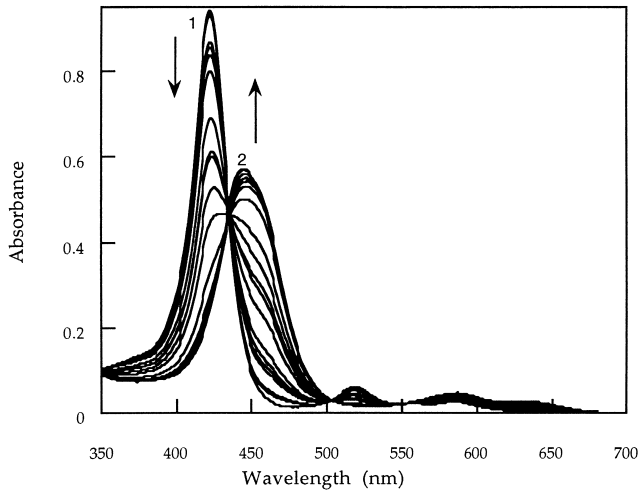

Fig. 3. Effect of Hg^{2+} addition to the TMPyP absorption spectrum ; (1) TMPyP solution, Soret band at 422 nm; (2) Hg-TMPyP complex, Soret band at 444 nm.

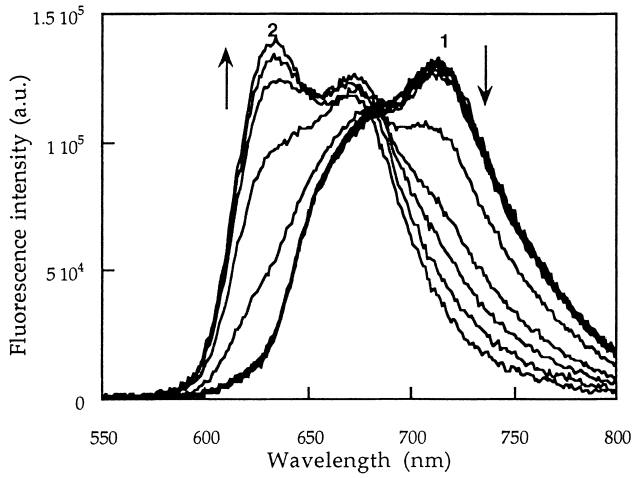

Fig. 5. Effect of the addition of Hg^{2+} on the fluorescence emission spectrum of TMPyP; (1) free base TMPyP, maximum at 720 nm; (2) Hg–TMPyP, complex, maximum at 632 nm.

[23] (Fig. 4). We can calculate the apparent equilibrium constant $K(Hg^{2+})$: $pK(Hg^{2+})=-5.7$. From (Fig. 4) we can also deduce the detection domain of Hg^{2+}:10^{-7}–8×10^{-6} mol/l.

Steady-state fluorescence experiments were carried out by varying $[Hg^{2+}]$ at pH=4. The 720 nm fluorescence band of TMPyP gradually disappears and a new band appears at 632 nm corresponding to Hg–TMPyP complex (Fig. 5). With main component analysis we find $pK(Hg^{2+})=-5.6$ and detection domain 10^{-7}–10^{-5} mol/l.

TMPyP and Hg–TMPyP differ by their fluorescence lifetimes (Fig. 6). We can fit the fluorescence decays of free base TMPyP and Hg–TMPyP complex by a mono-exponential: a 5.2 ns TMPyP and a 1.2 ns Hg–TMPyP lifetimes are measured. A main components analysis gives $pK(Hg^{2+})=-5.8$ and detection domain: 10^{-7}–10^{-5} mol/l.

The different spectroscopic methods used are in good agreement, and so, throughout these results we can conclude that it is possible to detect concentration of Hg^{2+} in the range 10^{-7}–10^{-5} mol/l. We also found the value of $pK(Hg^{2+})=-5.7+-0.1$.

Absorption and fluorescence lifetime allow ratiometric measurements.

3.1.2. *Sensitivity to others ions: Pb^{2+}, Cd^{2+}*

We have carried out the same experiments (absorption, steady-state and time-resolved fluorescence) for Pb–TMPyP and Cd–TMPyP complexes as for Hg^{2+}.

The results are summarized in Table 1.

Cd^{2+}, Pb^{2+}, Hg^{2+} sensing is possible using a water soluble porphyrin –TMPyP– thanks to characteristic wavelength bands in absorption or fluorescence emission, differ-

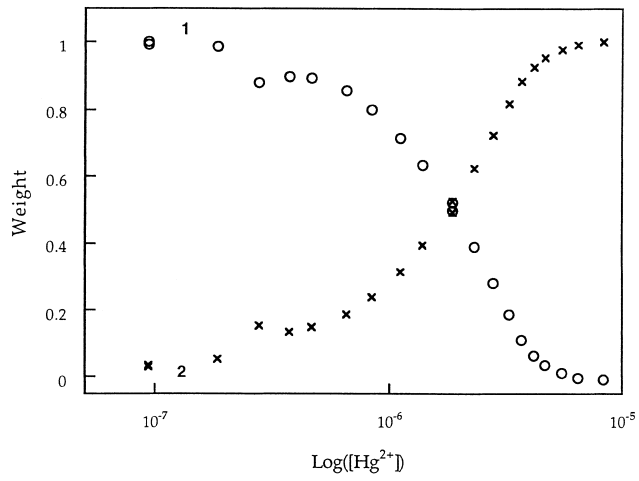

Fig. 4. A main component analysis of the absortion spectra of TMPyP+Hg^{2+} gives the weight of the two different forms, TMPyP and TMPyP-Hg as a function of $[Hg^{2+}]$; (1) weight of the free base TMPyP; (2) weight of the metallated TMPyP.

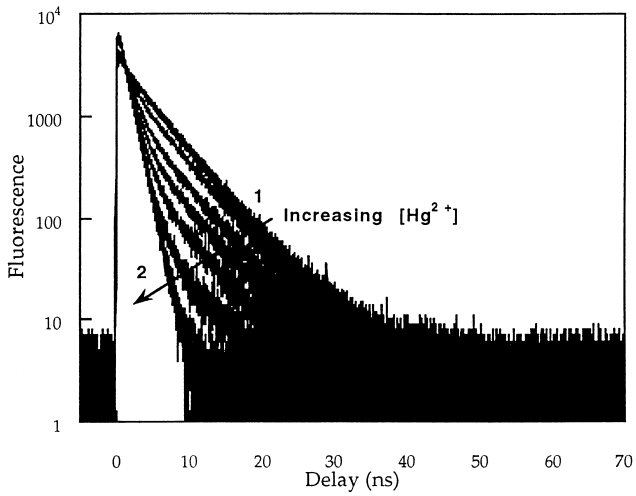

Fig. 6. Effect of the addition of Hg^{2+} on the time-resolved fluorescence decays; (1) free base TMPyP decay, 5.2 ns lifetime; (2) Hg–TMPyP complex, 1.2 ns lifetime.

Table 1
Systhesis of the results of the metallation of TMPYP with different metal ions in water

	λ Soret absorption (nm)	λ Fluorescence (nm)	λ Fluorescence lifetime (ns)	Apparent complexation constant p*K*	Detection limit (mol/l)
TMPyP	422	670–720	5.2		
Cd-TMPyP	447	620–670	1.2	5.2	10^{-1}–10^{-4}
Pb-TMPyP	480	[a]	[a]	4	10^{-5}–10^{-3}
Hg-TMPyP	444	632–670	1.2	5.7	10^{-1}–10^{-5}

[a] Non-fluorescent.

ent metal ions can be discriminated. In the special case of lead, the non-fluorescent complex allows a better sensitivity, even though the complexation constant is lower. In the case of mercury, the higher complexation constant can be due to the chelation out of the porphyrin core as reported previously [7]. The detection limits are better for mercury and cadmium than lead.

3.2. Experiments in sol–gel materials

By using TPPS in thin sol–gel films Czolk [10] found that the detection of Hg^{2+} was around 10^{-6} mol/l. We have used the TMPyP incorporated in thicker sol–gel materials (1 cm thickness), as described previously. In the sol–gel the Soret band shifts from 422 nm in solution to 433 nm. This result could be explained by an interaction of the cationic charges of the porphyrin and the negatively charged pore surface.

The sol–gel matrices containing TMPyP were exposed to different concentrations of mercury salt. In the first experiment 1 ml of 7.9×10^{-3} mol/l mercury acetate was added to the sol–gel material (3 ml volume). The disappearance of the 433 nm band and the appearance of the 458 nm band are observed (Fig. 7). The kinetic was carried out on this experiment. The advancement of the reaction can be defined by the relation:

$$\frac{A - A_0}{A_0},$$

where A is the 458 nm absorbance at time t, and A_0 the 458 nm initial absorbance. We plotted this expression as a function of time (Fig. 8). During the first 70 min, no change appeared in the Soret band.

The same experiment was carried out with a solution of lower concentration of mercury salt. In the case of a 2.3×10^{-3} mol/l Hg^{2+} solution, no effect was observed in the absorption spectrum. Concerning other ions no change appeared after 1 week on the Soret band of the porphyrins even for a concentration of 10^{-1} mol/l, this differs from the observation by Czolk.

The supernatant solution was analyzed after 1 day. The mercury salt concentration was found to be 10% of the starting concentration using the previous results in solution (Fig. 4). This can be explained by the diffusion of Hg^{2+} into the sol–gel matrix but without metallation of the porphyrin, the mercury interacting with the deprotonated silanol (–Si–O^-) at the pore surface. The induction period may correspond to the time of diffusion of salt and to the saturation of the deprotonated silanol (–Si–O^-) of the matrix, then the metallation of the porphyrins can occur.

The same experiments have been carried out with a sol–gel without porphyrins and the same percentage of mercury

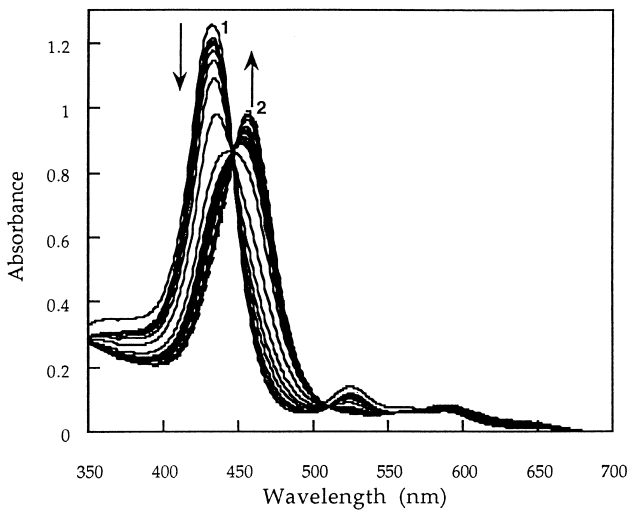

Fig. 7. Time effect of mercury diffusion in a TMPyP dopped sol–gel material $[Hg^{2+}]=7.9\times10^{-3}$ mol/l, $[TMPyP]=6\times10^{-7}$ mol/l; (1) t=0; maximum at 433 nm; (2) t=3 h; maximum at 458 nm.

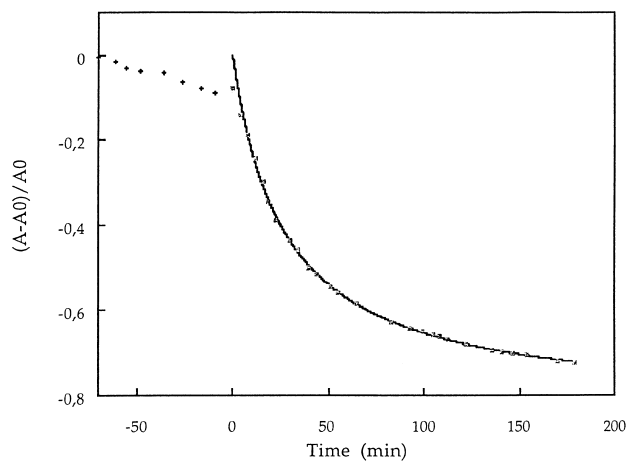

Fig. 8. Advancement of the TMPyP metallation with Hg^{2+} versus time.

salt have diffused in the matrix after 1 day. From the difference between 2.3×10^{-3} and 7.9×10^{-3} mol/l solutions we can deduce that the adsorption capacity of the sol–gel is 1.5×10^{-5} mol/ml of sol–gel.

3.3. Mercury detection with a TPyP monolayer

3.3.1. Spectroscopic study of a TPyP monolayer

Molecular layers of TPyP have been grafted on glass plates using the method described by Dequan Li [18,20]. A green coloration of the glass plate shows that the grafting was efficient. The absorbance is around 0.02 at the maximum of the Soret band (440 nm). In fluorescence the spectrum presents two bands: one at 661 nm and 720 nm for a 440 nm excitation. The time-resolved fluorescence decays can be fitted by a bi-exponential, therefore two lifetimes can be measured: 5 and 1.3 ns – the 5 ns lifetime represents a very minor contribution, the 1.3 ns lifetime can be explained by the protonation of the porphyrin during the grafting. The addition of sodium hydroxide leads to a blue shift of 9 nm of the Soret band (from 433 to 424 nm), this confirms that the porphyrin was protonated.

3.3.2. Mercury detection

The glass plates were dipped in solutions containing different concentrations of mercury salts (pH=5.6). A 15 nm red shift of the Soret band was observed (from 433 to 448 nm). This shift is smaller than the shift in solution (22 nm) and the one in sol–gel (25 nm). Fig. 9 represents the metallation degree of the porphyrin monolayer as a function of time. Equilibrium is reached within 30 min. The curves can be fitted by a mono-exponential function. Using a simple model of kinetics, we have plotted k (reaction rate constant) as a function of the mercury concentration. $k=k_{off}+k_{on}*[Hg^{2+}]$; with k_{on} the association rate constant and k_{off} the dissociation rate constant, (Fig. 10). We obtain a linear correlation with $k_{off}=0.0456\ s^{-1}$ and $k_{on}=506$ l/mol/s. The detection limit is 10^{-6} mol/l of mercury. The calibration curve of our system has been established by reporting the reaction advancement at the equilibrium as a function of the logarithm of the Hg^{2+} concentration (Fig. 11). From k_{off} and k_{on} we can evaluate the association constant $pK(Hg^{2+})=-4$.

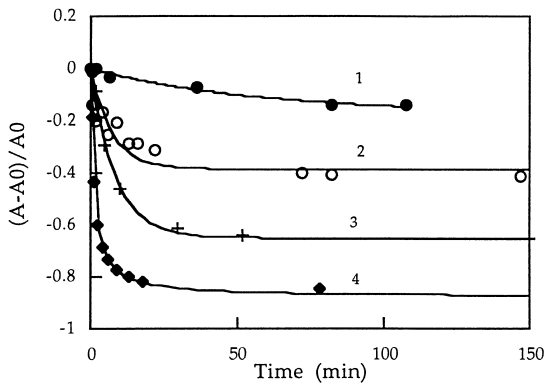

Fig. 9. Advancement of the metallation as a function of time after the addition of Hg^{2+}: (1) 10^{-6}; (2) 10^{-5}; (3) 10^{-4}; (4) 10^{-3} mol/l.

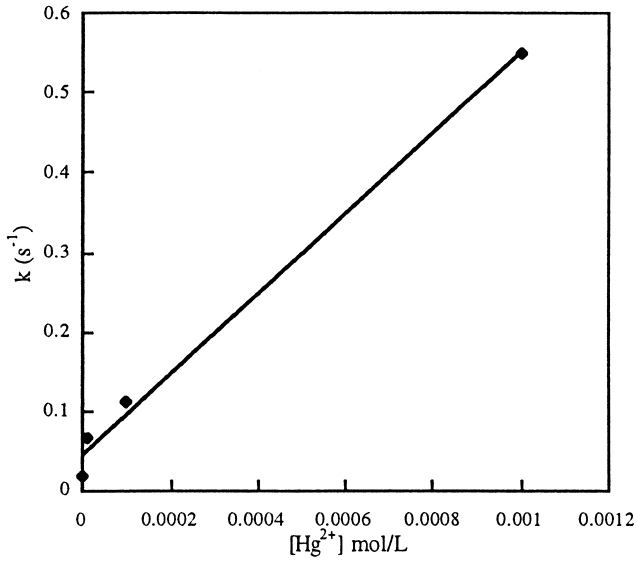

Fig. 10. Reaction rate constant as a function of $[Hg^{2+}]$.

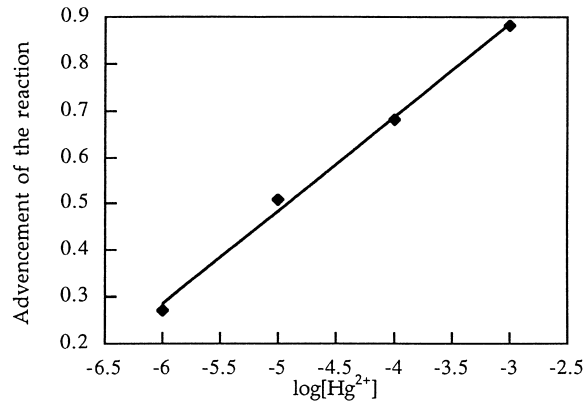

Fig. 11. Calibration curve for Hg^{2+} detection with a porphyrin monolayer.

4. Conclusion

The study of the metallation of the porphyrins in solution has emphasized the formation of 1:1 complex for each ion with a constant of complexation depending on the nature of the ions. The strongest effects were observed for mercury due to the specific interaction of this metal with the porphyrin. But in sol–gel matrices and particularly in bulk materials, the metallation was very difficult due to a strong interaction between the salt and $-O^-$ at the pore surface. Meanwhile, the salt diffused in the sol–gel and we can observe the accumulation of salt in the sol–gel. These particular materials could be used to purify water as a filter. It acts like a sponge of ions. A new structure is investigated

in the laboratory to limit the interaction between the $-O^-$ and the salt but also to increase the sensitivity and the kinetics. Porphyrin monolayers allow faster detection and better sensitivity in comparison with the sol–gel material. New development of porphyrin multilayers are now in progress in our laboratory.

References

[1] J. Rodier, Dunod edition, Analyse de l'eau (1996) 310.
[2] I. Leray, M.C. Vernieres, R. Loucif-Saibi, C. Bied-Charreton, J. Faure, Sensors & Actuators 36 (1996) 67.
[3] M. Tabata, J. Nishimoto, A. Ogata, T. Kusano, N. Nahar, Bull. Chem. Soc. Jpn. 69 (1996) 673.
[4] S.A. Azim, M.A. El-Kemary, S.A. El-Daly, H.A. El-Daly, M.E. El-Khouly, E.M. Ebid, J. Chem. Soc., Faraday Trans. 92 (1996) 747.
[5] J.A. Schneider, J.F. Hornig, Analyst 118 (1993) 933.
[6] R. Giovannetti, V. Bartocci, Talanta (1998) 977.
[7] R. Czolk, R. Reichert, H.J. Ache, Sensors & Actuators B 7 (1992) 540.
[8] A. Morales-Bahnik, R. Czolk, J. Reichert, H.J. Ache, Sensors & Actuators B 13 14 (1993) 424.
[9] M. Plaschke, R. Czolk, H.J. Ache, Anal. Chim. Acta 304 (1995) 107.
[10] P. Battioni, E. Cardin, M. Louloudi, B. Schollhorn, G.A. Sphyroulias, D. Mansuy, T.G. Traylor, J. Chem. Soc., Chem. Comm. (1996) 2037.
[11] X.-J. Wang, L.M. Yates III, E.T. Knobbe, J. Lumin. 60 61 (1994) 469.
[12] A.K. Sinha, B. Bihari, B.K. Mandal, L. Chen, Macromolecules 28 (1995) 5681.
[13] H. Inoue, T. Iwamoto, A. Makishima, M. Ikemoto, K. Horie, J. Opt. Soc. Am. B 9 (1992) 816.
[14] A.V. Veret-Lemarinier, J.P. Galaup, A. Ranger, F. Chaput, J.P. Boilot, J. Lumin. 64 (1995) 223.
[15] D.D. Dunuwila, B.A. Torgeson, C.K. Chang, K.A. Berlund, Anal. Chem. 66 (1994) 2743.
[16] G.E. Badini, K.T.V. Grattan, A.C.C. Tseung, Analyst 120 (1995) 1028.
[17] S.K. Lee, I. Okura, Analyst 122 (1997) 81.
[18] D. Li, B.I. Swanson, J.M. Robinson, M.A. Hoffbauer, J. Am. Chem. Soc. 115 (1993) 6975.
[19] R.F. Pasternack, P.R. Huber, P. Boyde, G. Engasser, L. Francesdoni, E. Gibbs, P. Fasella, G.C. Venturo, L. de C. Hinds, J. Am. Chem. Soc. 94 (1972) 4511.
[20] D. Li, C.T. Buscher, B.I. Swanson, Chem. Mater. 6 (1994) 803.
[21] F. Devreux, J.P. Boilot, F. Chaput, A. Leconte, Phys. Rev. A 41 (1990) 6901.
[22] L. Schoutteten, P. Denjean, R.B. Pansu, J. Fluoresc. 7 (1997) 155.
[23] S. Kawata, H. Komeda, K. Sasaki, S. Minami, Appl. Spectrosc. 4 (1985) 610.